Pergamon

Int. J. Heat Mass Transfer. Vol. 37, No. 14, pp. 2131–2137, 1994

0017-9310/94 $7.00+0.00

0017-9310(94)E0063-Z

The influence of heat transfer on the formation of hydrate layers in pipes

FRANK DORSTEWITZ and DIETER MEWES
Institute of Process Engineering, University of Hannover, Callinstr. 36, D-30167 Hannover, Germany

(*Received* 20 *December* 1993)

Abstract—Experiments are performed in order to study the effect of hydrate formation on heat transfer in pipes. The hydrate formation in the horizonal flow of the gaseous refrigerant R134a and water is examined in a transparent test section at low pressure. The experiments conducted have shown that the formation of hydrates starts on the pipe wall. The whole perimeter of the pipe wall is covered by hydrates and a hydrate layer is achieved. The thickness of the hydrate layer can be related to the measured heat transfer resistances and measured pressure losses. The thickness of the hydrate layer can be calculated analytically, if a first-order logarithmic function of the radial coordinate is assumed for the temperature field within the hydrate layer.

1. INTRODUCTION

UP TO now, crude oil and natural gas from subsea reservoirs are exploited by conveying the mixture of oil, gas, aqueous brine and entrained solids from the well along risers to the processing platforms, where the different phases of the well stream mixture are separated. Oil and gas as unprocessed materials are conveyed to the shore by pipeline or by tankers. The investment and operating costs of this kind of exploitation are high. The exploitation of marginal gas fields is not economical yet. Developing these fields from already existing platforms offers a possibility for reducing costs. This has resulted in the idea that it may be possible to develop marginal fields by full well stream transfer tying back to already existing platforms. In this case the multiphase mixture has to be conveyed without further processing to the platform or even to shore.

This technology handles multiphase flows over long distances in cold environments. The temperature of the multiphase mixture decreases along the pipe due to the low temperature of the surrounding sea water. If the temperature in the pipeline is low enough, hydrate formation may occur. The design of multiphase transmission systems requires a detailed know-ledge of the heat and mass transfer in multiphase flow with hydrate formation.

To distinguish the flow conditions for hydrate deposition the mutual effects of hydrate formation, fluid dynamics and heat and mass transfer have to be examined. Therefore a model system is chosen, that enables the study of hydrate formation in a low pressure, transparent test section. The used gas is the refrigerant R134a.

2. HYDRATES

Hydrates are solid, crystalline compounds of water and low boiling gases forming a special form of molecular structure. Because of their hydrogen bonding properties, the water molecules are able to form cavities, which can accommodate low molecular weight molecules. The inclusion of these gas molecules stabilizes the metastable water lattice structure. There are two different types of common hydrate structure, which are referred to as structure I and structure II. Both structures contain numerous small and large cavities. Only molecules of modest size and appropriate geometry are able to enter the cavities.

The hydrate of R134a is of structure II. A unit cell of this hydrate structure with its cavities is shown in Fig. 1. The unit cell is composed of 136 water molecules. The water molecules form 16 small and 8 large cavities. The diameter of the smaller cavities is 0.49 nm, while the diameter of the large cavities is 0.65 nm [1]. The maximum molecular length of the refrigerant R134a is 0.64 nm [2]. Therefore, R134a stabilizes the large cavities in a structure II hydrate, where the introduced molecules occupy the large cavities while smaller cavities remain unoccupied.

The phase behavior of R134a and water is illustrated in Fig. 2. This figure shows a p–T-phase diagram for hydrates of R134a. The points of the fully drawn curve are three phase loci. The curve represents equilibria between hydrate, R134a in gaseous form and liquid water. The curve is approximated by the equation:

$$\ln(p) = a + \left(\frac{b}{T}\right) + c \ln(T), \qquad (1)$$

NOMENCLATURE

a	thermal diffusivity [$m^2 s^{-1}$]
a, b, c	constants
Bi	Biot number
c_p	specific heat capacity [$J kg^{-1} K^{-1}$]
d	diameter [m]
Δh	specific formation enthalpy [$J kg^{-1}$]
l	length [m]
p	pressure [Pa]
Δp	pressure loss [Pa]
Ph	phase change number
r	radius [m]
s	thickness of the hydrate layer [m]
T	temperature [K]
t	elapsed time [s]
U	overall heat transfer coefficient [$W m^{-2} K^{-1}$]
$\dot{V}$	volumetric flow rate [$m^3 s^{-1}$].

Greek symbols

α	heat transfer coefficient [$W m^{-2} K^{-1}$]
λ	thermal conductivity [$W m^{-1} K^{-1}$]
ρ	density [$kg m^{-3}$]
τ	dimensionless time
θ	dimensionless function of heat fluxes.

Subscripts

2ph	two phase
c	cooling agent
eq	equilibrium
g	gas
h	hydrate
o	outer
w	water
wall	wall.

where p is the equilibrium pressure (MPa), T the equilibrium temperature (K) and a, b, c are constants given by Oowa *et al.* [3]. They are listed in Table 1. The data points displayed, are hydrate equilibria measured by Dorstewitz and Mewes [4]. The deviation between this observed pressures and the pressures calculated by equation (1) is within 4%.

3. EXPERIMENTAL SET-UP

Hydrate formation was studied experimentally in a horizontal pipe flow of gas and water. A schematic description of the test facility used is given in Fig. 3. Water as the liquid phase and the gaseous refrigerant are pumped from storage tanks into the test section. The pressure, the temperature and the volumetric flow rate of each fluid are measured. The tubing is made of glass with an inner diameter of $d_i = 15$ mm. The cooling is obtained by a jacket tube in countercurrent flow arrangement. The test section is composed of an entrance section with an l/d ratio of 135 and an approximately 2 m long measurement section.

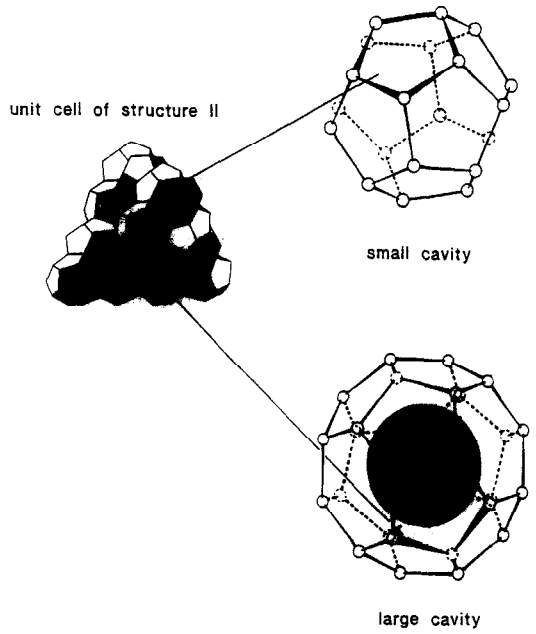

FIG. 1. The unit cell of the structure II hydrate with its cavities.

The system pressure and pressure loss in the measurement section as well as the temperature of the two-phase mixture at the entrance and the exit are measured. Finally a separator is connected which gravitionally separates the water and the gas. Hydrate particles carried along with the water are separated in a filter, if necessary. The separation step is required to allow for the recirculation of the phases. The pressure in the system is $p = 0.12$ MPa. The volumetric flow rate of water is varied in the range of $0.5 \leqslant \dot{V}_w \leqslant 1.5$ l min^{-1} and the volumetric flow rate of R134a is varied in the range of $1.5 \leqslant \dot{V}_g \leqslant 4.3$ l min^{-1}.

At the end of the test section a viewing system for axial photography of the flow is installed. The development and the application of axial flow viewing systems is described in detail by Hewitt and Whalley [5]. The used axial flow view photographic system is depicted in Fig. 4. The multiphase flow is passing the horizontal measurement section. A short section of the jacket tube is illuminated. The illuminated cross-

Table 1. Constants in equation (1) for R134a [3]

a	b	c
-8.1079×10^2	1.9560×10^4	1.3122×10^2

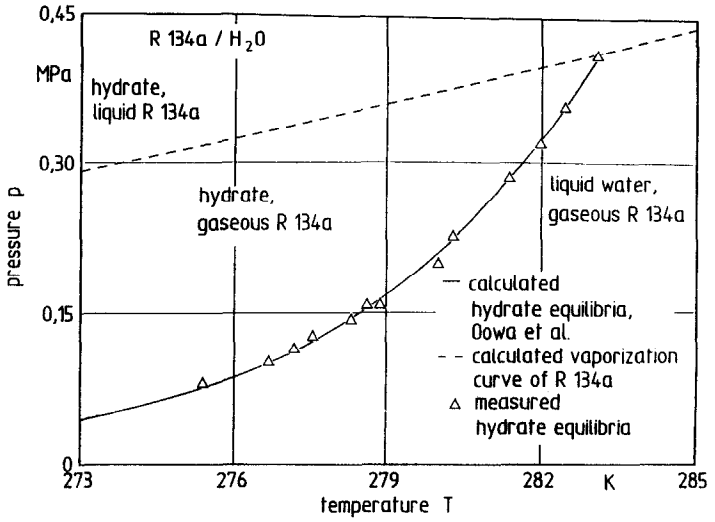

FIG. 2. p–T-phase diagram for water and R134a.

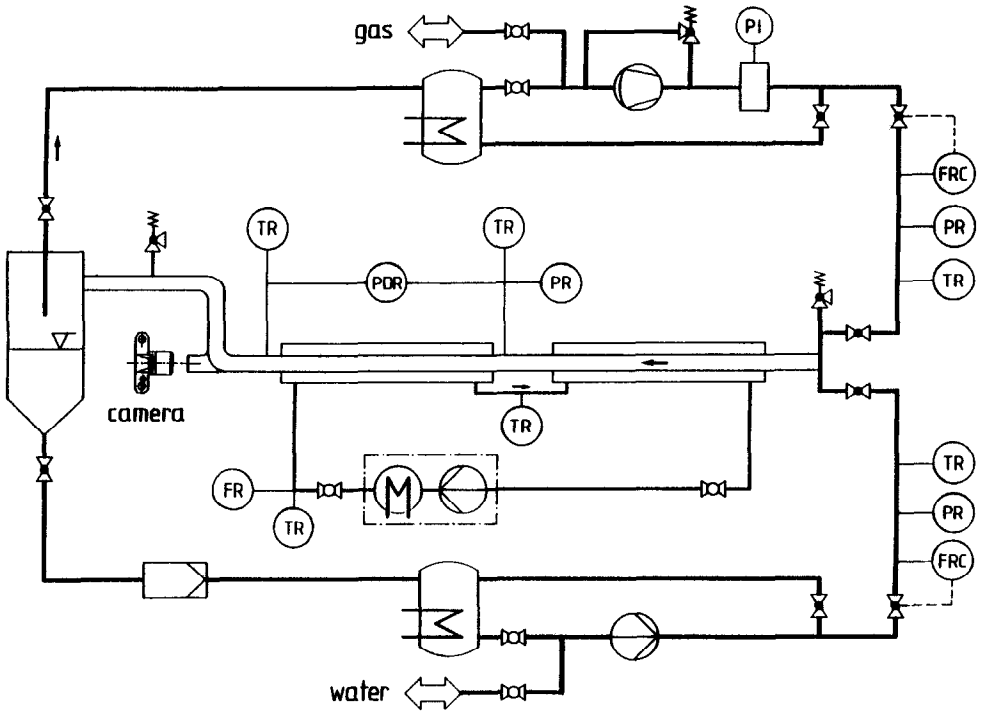

FIG. 3. Experimental set-up.

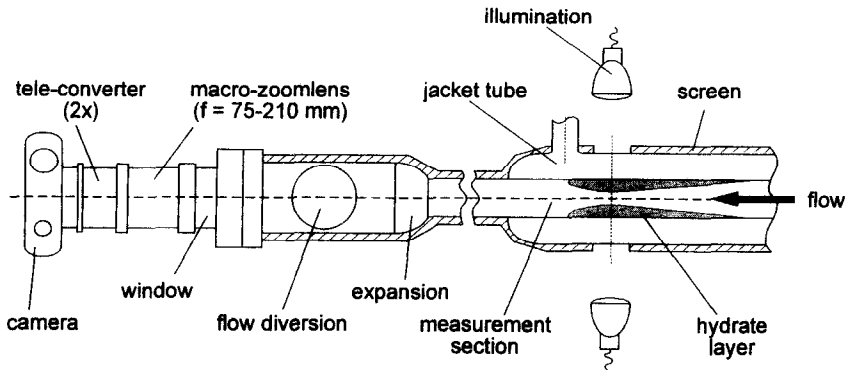

FIG. 4. Axial flow view photographic system.

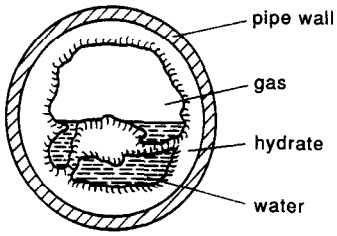

FIG. 5. Hydrate formation pattern in the 15 mm test pipe.

section within the measurement section can be viewed through a window at the end of the system. A photocamera with its lens system is mounted concentrically with the tubing. The camera if focused on the plane of illumination. The fluids passing the tubing are diverted 90° in a T-fitting, which is connected to the enlargement behind the plane of illumination.

Using the axial view technique, it is possible to obtain one cross-section of a stratified flow with hydrate formation. The circumferential distribution of the hydrates can be clearly seen and the formation as well as the deposition of hydrates within the illuminated section are observed. Furthermore it is possible to measure the thickness of the growing hydrate layer within the plane of illumination.

4. RESULTS

4.1. *Hydrate formation*

The appearance of the hydrates in the pipeline is illustrated in Fig. 5. The formation of a plug starts on the pipe wall where the interface between water and gas is located. The whole perimeter of the wall is covered by hydrates and a closed hydrate layer is achieved. The hydrate layer grows radially towards the center of the pipe.

4.2. *Pressure loss*

The time-plot of the related pressure loss is illustrated in Fig. 6. The system pressure is $p = 0.128$ MPa. Hence hydrates can form at temperatures below $T_{eq} = 277.43$ K. The flow regime is plug flow. Due to the void distribution, the value of the related pressure loss is low. The onset of hydrate formation after 121 min leads to fluctuations in the pressure loss history.

With an increasing hydrate layer the free cross-sectional area decreases by the power of two. This leads to a nearly parabolic increase of the measured pressure loss up to the plugging of the pipe after 129 min.

If a turbulent flow of a homogeneous mixture of gas and water is assumed, the mean thickness of the hydrate layer can be calculated directly from the measured pressure loss:

$$\left(\frac{\Delta p}{\Delta l}\right)_{2ph,0} \Big/ \left(\frac{\Delta p}{\Delta l}\right)_{2ph,h} = \left(\frac{d_i - 2s}{d_i}\right)^{4.75}. \qquad (2)$$

4.3. *Heat transfer*

The growing hydrate layer implies an increasing resistance for heat conduction to the pipe wall. For constant fluid conditions at the entrance of the measurement section, the change of the heat transfer resistance can be calculated from the measured fluid temperature at the exit. The difference in the heat transfer resistances for the surface covered by hydrates and for the clean surface is known as the fouling factor

$$\frac{1}{U_i} - \frac{1}{U_{i,0}} = \frac{d_i}{2\lambda_h}\left[\ln\left(\frac{d_i - 2s}{d_i}\right)\right]^{-1}. \qquad (3)$$

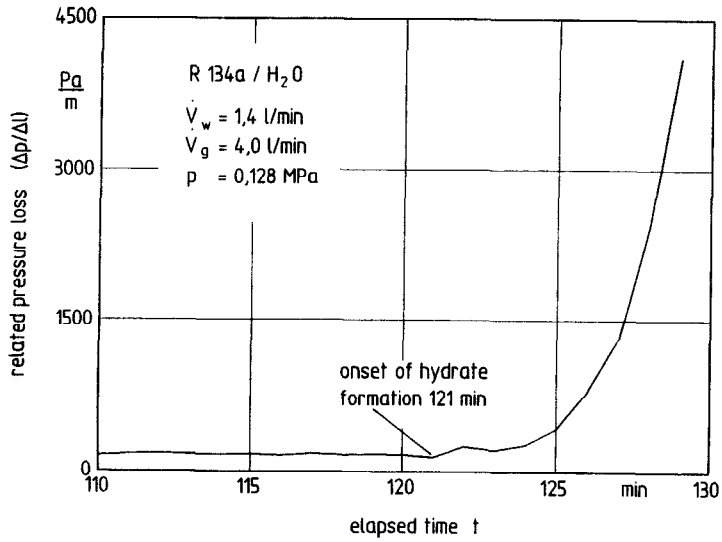

FIG. 6. Measured pressure loss for hydrate formation in the 15 mm test pipe.

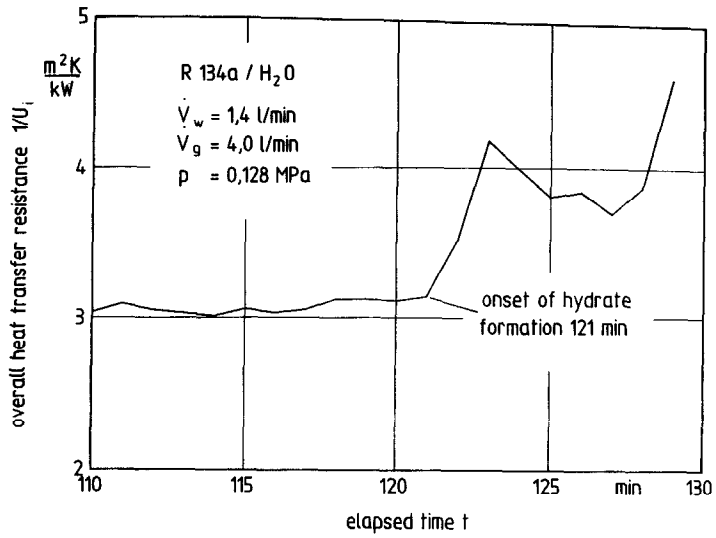

FIG. 7. Measured heat transfer resistance for hydrate formation in the 15 mm test pipe.

If no solid removal takes place, U_i will increase with time and the pipeline will be plugged.

Figure 7 shows the measured heat transfer resistance $1/U_i$ vs time for turbulent flow conditions. After an elapsed time of $t = 121$ min a hydrate layer is observed on the pipe wall. The measured heat transfer resistances increase. The liquid slugs flowing through the pipe are able to clean the pipe wall for 3 min. This phenomenon results in a decreasing heat transfer resistance. The further hydrate removal is not as high as the hydrate deposition. This results in an increasing thickness of the hydrate layer and an increasing heat transfer resistance.

4.4. *Hydrate layer*

In Fig. 8 the formation of a thin hydrate layer is illustrated schematically. It is assumed that the thickness of the hydrate layer is small relative to the pipe diameter. With this assumption the inner heat transfer coefficient α_i is not greatly affected and can be assumed to be constant. The outer combined heat transfer coefficient:

$$\frac{1}{U_o} = \frac{d_i \ln\left(\frac{d_o}{d_i}\right)}{2\lambda_{wall}} + \frac{1}{\alpha_o}\frac{d_i}{d_o}, \tag{4}$$

is fixed by the processing conditions. The governing equation for this layer, is the conduction equation. Integrating the conduction equation with respect to r from r_f to r_i yields:

$$\frac{d}{dt}\int_{r_f}^{r_i} rT(r,t)\,dr + r_f\frac{dr_f(t)}{dt} - a_h\left[r_i\frac{\partial T(r_i,t)}{\partial r} - r_f\frac{\partial T(r_f,t)}{\partial r}\right] = 0. \tag{5}$$

Three boundary conditions exist for this problem, which are:

$$T(r_f,t) = T_{eq}, \tag{6}$$

$$-\lambda_h\frac{\partial T(r_i,t)}{\partial r} = U_o[T(r_i,t) - T_c], \quad \text{and} \tag{7}$$

$$\lambda_h\frac{\partial T(r_f,t)}{\partial r} + \alpha_i[T_{2ph} - T(r_f,t)] = \rho\Delta h\frac{dr_f}{dt}. \tag{8}$$

If a first-order logarithmic function of the radial coordinate r is assumed for the temperature field within the hydrate layer, the integral equation for

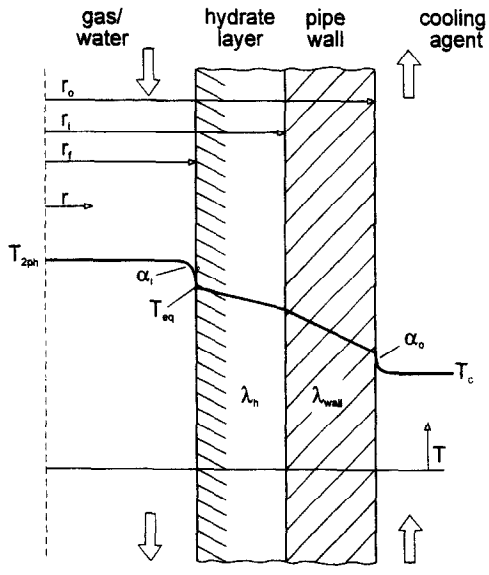

FIG. 8. Formation of a thin hydrate layer.

the hydrate layer will become a non-linear ordinary differential equation [6]. This equation is:

$$\left(\frac{\frac{Bi_r^2}{2}\left(\frac{1}{Bi_r}+\frac{1}{2}\right)-\frac{Bi^2}{4}}{\left[\ln\left(\frac{Bi_r}{Bi}\right)+\frac{1}{Bi_r}\right]^2}\right.$$

$$\left.+Bi^2\left\{Ph-\frac{\frac{1}{2}}{\left[\ln\left(\frac{Bi_r}{Bi}\right)+\frac{1}{Bi_r}\right]}\right\}\right)\frac{dBi}{d\tau}$$

$$-Bi\,Ph\left\{Bi\,\theta-\frac{1}{\left[\ln\left(\frac{Bi_r}{Bi}\right)+\frac{1}{Bi_r}\right]}\right\}=0, \quad (9)$$

in dimensionless form, where two Biot numbers are defined, the Biot number Bi for the dimensionless flow radius and the Biot number Bi_r for the dimensionless radius of the pipe:

$$Bi \equiv \frac{r_f U_o}{\lambda_h} \quad \text{and} \quad Bi_r \equiv \frac{r_i U_o}{\lambda_h}. \quad (10)$$

The dimensionless solid–liquid phase line, the Biot number Bi, is a function of the Biot number Bi_r and three additional dimensionless parameters, which are the dimensionless time τ and the phase change number Ph:

$$\tau \equiv \frac{U_o^2 a_h}{\lambda_h^2 Ph} t \quad \text{and} \quad Ph \equiv \frac{\Delta h}{c_p(T_{eq}-T_c)}, \quad (11)$$

and the dimensionless parameter θ:

$$\theta \equiv \frac{\alpha_i}{U_o}\left(\frac{T_{2ph}-T_c}{T_{eq}-T_c}-1\right). \quad (12)$$

θ is the ratio of the two heat fluxes. The parameters Bi_r and θ are process design parameters, while Ph is a material parameter. The governing equation (9) for the Biot number as a function of the dimensionless time τ is solved using the Runge–Kutta integration scheme.

The results for the thus calculated Biot numbers as a function of the dimensionless time τ are presented in Fig. 9. The measured Biot numbers are in good agreement for $\tau < 0.5$. If the thickness of the hydrate layer increases, the free cross-sectional area will decrease. This leads to an increasing inner heat transfer coefficient α_i for constant volumetric flow rates of gas and water. Due to the increasing inner heat transfer coefficient the combined parameter θ increases. This results in a more slowly growing hydrate layer. Therefore the measured values for the Biot numbers are higher than the calculated values. The numerical solution indicates that for the given parameters a stable thickness of the hydrate layer is not achieved and the pipeline will be plugged, $Bi = 0$.

Acknowledgements—The financial support of this work by the German Federal Ministry of Research and Technology is gratefully acknowledged. We would also like to thank the Solvay Deutschland GmbH for providing us with R134a.

REFERENCES

1. E. Sloan, Natural gas hydrates phase equilibria and kinetics: understanding the state-of-the-art, *Revue Inst. Français Pétrole* **45**, 245–266 (1990).
2. F. Isobe and Y. H. Mori, Formation of gas hydrates or ice by direct-contact evaporation of CFC alternatives, *Int. J. Refrig.* **15**, 137–142 (1992).

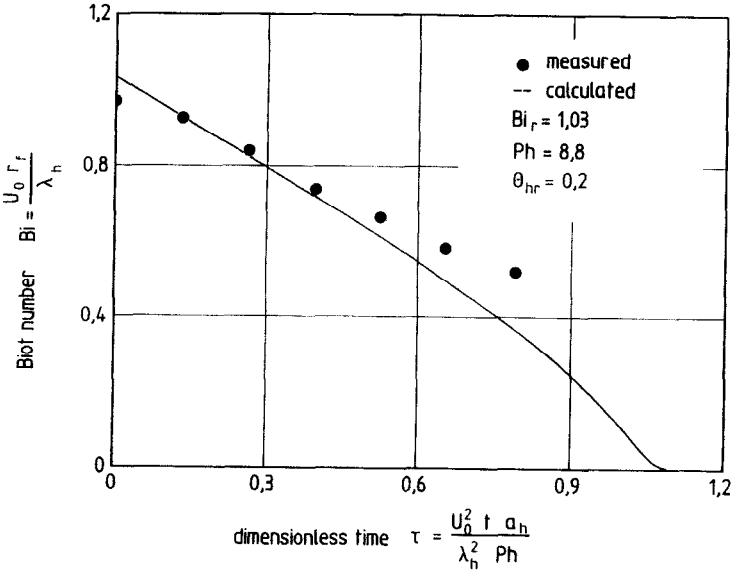

FIG. 9. Calculated and measured Biot numbers.

3. M. Oowa, M. Nakaiwa, T. Akiya, Fukuura, K. Suzuki and M. Ohsuka, Formation of CFC alternative R134a gas hydrate, *Proceedings of the 25th AIChE Intersoc. Energy Conversion Engineering Conference*, Vol. 4, pp. 269–274. Reno (1990).
4. F. Dorstewitz and D. Mewes, Thermodynamische Gleichgewichte beim Bilden von Hydraten aus R12 und R134a, *Chem.-Ing.-Tech.* **64,** 466–467 (1992).
5. G. Hewitt and P. B. Whalley, Advanced optical instrumentation methods, *Int. J. Multiphase Flow* **6,** 139–156 (1980).
6. H. Wang and E. M. Perry, Criteria for achieving a stable solidified layer inside a nozzle using integral solutions. In *Collected Papers in Heat Transfer* (Edited by K. T. Yang), ASME HTD-Vol. 104, pp. 129–135. ASME, New York (1988).